Acta Mechanica Sinica (2018) 34(4):623–631
https://doi.org/10.1007/s10409-018-0756-1

RESEARCH PAPER

An efficient unstructured WENO method for supersonic reactive flows

Wen-Geng Zhao[1] · Hong-Wei Zheng[2,3] · Feng-Jun Liu[4] · Xiao-Tian Shi[1] · Jun Gao[1] · Ning Hu[1] · Meng Lv[1] · Si-Cong Chen[1] · Hong-Da Zhao[5]

Received: 2 September 2017 / Revised: 23 October 2017 / Accepted: 27 November 2017 / Published online: 15 March 2018
© The Chinese Society of Theoretical and Applied Mechanics; Institute of Mechanics, Chinese Academy of Sciences and Springer-Verlag GmbH Germany, part of Springer Nature 2018

Abstract
An efficient high-order numerical method for supersonic reactive flows is proposed in this article. The reactive source term and convection term are solved separately by splitting scheme. In the reaction step, an adaptive time-step method is presented, which can improve the efficiency greatly. In the convection step, a third-order accurate weighted essentially non-oscillatory (WENO) method is adopted to reconstruct the solution in the unstructured grids. Numerical results show that our new method can capture the correct propagation speed of the detonation wave exactly even in coarse grids, while high order accuracy can be achieved in the smooth region. In addition, the proposed adaptive splitting method can reduce the computational cost greatly compared with the traditional splitting method.

Keywords Supersonic reactive flows · Adaptive splitting scheme · Unstructured grids · WENO reconstruction

1 Introduction

During the last several decades, numerical simulation has been applied to supersonic reactive flows [1–14] and plays an increasingly important role. However, there are still some challenges in the simulation of supersonic reactive flow [15]. A well-known difficulty [16–21] is unphysical wave speeds, which are caused by the stiffness of the source term. This numerical phenomenon was first observed by Colella et al. [22]. Later, LeVeque and Yee [23] found that the propagation error is due to the numerical viscosity in the solution of the convective terms, which smears the discontinuity front. Various strategies have been proposed to overcome this difficulty [24–32], for example, the random projection method [11–13], modified fractional step method [14], Min-Max method [15], arbitrary high order derivatives (ADER) method [16], sub-cell resolution method [17], and equilibrium state method [18]. Even though these methods can prevent the incorrect propagation speed of discontinuities efficiently, most of these simulations are restrained within the structured grids and cannot be extended to the unstructured grid straightforward [33–37]. In Ref. [38], Togashi applied the monotonic upwind scheme for conservation laws (MUSCL) to unstructured grids and found that the simulations using unstructured grids require many more cells than structured grids to obtain the same result. To get a more accurate result in unstructured grids, we can employ a high-order accurate numerical method instead of the traditional second-order numerical method. In fact, there are many high-order numerical methods [39,40] developed in the past decades: the essentially non-oscillatory method (ENO) [41], the weighted ENO (WENO) method [42–48], the discontinuous Galerkin method [39,49,50], and the spectral volume method [51]. However, the unstructured high-order accurate methods for supersonic reactive flow [52–67] are still rarely conducted because of the complicated topology of unstructured grid, stiffness of governing equation and complexity of the reaction model.

The purpose of this article is to propose an efficient, unstructured high-order accurate method for supersonic reac-

✉ Wen-Geng Zhao
zhaowengeng12@126.com

✉ Xiao-Tian Shi
xxtshi@163.com

1 China Academy of Aerospace and Aerodynamics, Beijing 100074, China

2 LHD, Institute of Mechanics, CAS, Beijing 100190, China

3 School of Engineering Science, University of Chinese Academy of Sciences, Beijing 100049, China

4 AECC Beijing Institute of Aeronautical Materials, Beijing 100095, China

5 Science and Technology on Scramjet Laboratory, Beijing Power Machinery Research Institute, Beijing 100074, China

tive flows. In the proposed method, we use an operator splitting scheme to solve the convection term and reaction source term separately. In the reaction step, an adaptive time-step method is developed, which can improve the efficiency greatly compared to the traditional splitting method. In the convection step, an unstructured third-order accurate WENO finite volume method (FVM) is adopted to obtain high order special discretization.

The outline of this paper is described as follows. The governing equations for supersonic reactive flows and chemical models are given in Sect. 2. The adaptive time-step method in reaction step and unstructured WENO reconstruction for convection step is introduced in Sect. 3. Numerical experiments are presented in Sect. 4. And Sect. 5 is devoted to the conclusion.

2 Governing equation and chemical models

The hyperbolic conservation laws with source term are used to model the supersonic reaction flow. Neglecting the viscosity and heat transfer, the governing equation can be written as

$$\frac{\partial \boldsymbol{u}}{\partial t}+\frac{\partial \boldsymbol{F}}{\partial x}+\frac{\partial \boldsymbol{G}}{\partial y}=\boldsymbol{S}, \tag{1}$$

where $\boldsymbol{u}, \boldsymbol{F}, \boldsymbol{G}$ and $\boldsymbol{S}$ are the state vector of conservative variables, the flux vector in x-direction, the flux vector in y-direction and the source term. The expression of the source term will vary with the chemical reaction models. Two common chemical reaction modes in numerical simulation have been included in this work: the one-step reaction model [11–18] and detailed reaction model [24–32].

2.1 One-step reaction model

The one-step reaction model is the simplest reaction model, in which there are only two states for mixture: burnt gas and un-burnt gas. In the one-step reaction model, the conserved variables $\boldsymbol{u}$, flux vector $\boldsymbol{F}$, $\boldsymbol{G}$ and source term $\boldsymbol{S}$ in Eq. (1) can be expressed as follows

$$\boldsymbol{u}=\begin{pmatrix}\rho\\ \rho u\\ \rho v\\ E\\ \rho z\end{pmatrix},\quad \boldsymbol{F}=\begin{pmatrix}\rho u\\ \rho u^2+p\\ \rho uv\\ u\left(E+p\right)\\ \rho uz\end{pmatrix},$$
$$\boldsymbol{G}=\begin{pmatrix}\rho v\\ \rho uv\\ \rho v^2+p\\ v\left(E+p\right)\\ \rho vz\end{pmatrix},\quad \boldsymbol{S}=\begin{pmatrix}0\\ 0\\ 0\\ 0\\ -K\left(T\right)\rho z\end{pmatrix}, \tag{2}$$

where ρ is the mixture density, u and v are the velocities in x- and y-direction, E is the mixture total energy, and z is the mass fraction. $K(T)$ is the chemical reaction rate, which can be expressed in the Arrhenius form or Heaviside form. The pressure p is given by

$$p=(\gamma-1)\left[E-\frac{1}{2}\rho\left(u^2+v^2\right)-q_0\rho z\right], \tag{3}$$

where q_0 is the chemical heat released in the reaction. For the calorically perfect gas, the temperature T is defined as

$$T=\frac{p}{\rho}. \tag{4}$$

2.2 Detailed reaction model

The detailed reaction model takes the process of chemical reaction kinetics into consideration and usually can be represented in the general form as follows.

$$\sum_{i=1}^{ns} v'_{i,j}B_i \Leftrightarrow \sum_{i=1}^{ns} v''_{i,j}B_i,\ j=1,2,\ldots,nr, \tag{5}$$

where ns is the number of species and nr is the number of reactions. In the detailed reaction model, the conserved variables $\boldsymbol{u}$, flux vector $\boldsymbol{F}$, $\boldsymbol{G}$ and source term $\boldsymbol{S}$ in Eq. (1) can be expressed as follows.

$$\boldsymbol{u}=\begin{pmatrix}\rho\\ \rho u\\ \rho v\\ E\\ \rho z_1\\ \vdots\\ \rho z_{ns-1}\end{pmatrix},\quad \boldsymbol{F}=\begin{pmatrix}\rho u\\ \rho u^2+p\\ \rho uv\\ u\left(E+p\right)\\ \rho uz_1\\ \vdots\\ \rho uz_{ns-1}\end{pmatrix},$$
$$\boldsymbol{G}=\begin{pmatrix}\rho v\\ \rho uv\\ \rho v^2+p\\ v\left(E+p\right)\\ \rho vz_1\\ \vdots\\ \rho vz_{ns-1}\end{pmatrix},\quad \boldsymbol{S}=\begin{pmatrix}0\\ 0\\ 0\\ 0\\ \omega_1\\ \vdots\\ \omega_{ns-1}\end{pmatrix}, \tag{6}$$

where ω_i is the production rate for the ith species. For the calorically perfect gas, specific heat is constant and the temperature can be obtained according to Eq. (4). For the thermally perfect gas, specific heats are usually given by fitting polynomial [42] and Newton iteration is applied to compute the temperature from the conserved variables.

3 Numerical method

In this section, an adaptive time step method in the reaction step and the unstructured WENO reconstruction in the convection step are stated in detail. We solve these governing equations using the Strang splitting scheme

$$U^{n+1} = C\left(\frac{\Delta t}{2}\right) R\left(\Delta t\right) C\left(\frac{\Delta t}{2}\right) U^{n}, \tag{7}$$

where C and R represent the convection operator and the reaction operator, respectively. In the reaction step, the third-order total variation diminishing (TVD) Runge–Kutta time discretization with adaptive time step is employed. In the convection step, the unstructured WENO reconstruction is used.

3.1 Adaptive time step method in reaction step

An essential characteristic for supersonic reactive flow is radical chemical reactions whose relaxation times are orders of magnitude smaller than the typical time scale of transport phenomena, which is usually called stiffness [2,14]. In the supersonic reactive flows, the stiff source term leads to severe time-step limitations for a numerical scheme, which is far beyond the Courant–Friedrichs–Lewy (CFL) stability restriction to solve. Even though the implicit scheme can reduce the stiffness effectively, the inverse of Jacobian matrix for the source term is needed, which takes great computational time in the detailed reaction model. In addition, the accuracy of an implicit scheme is low, which may spoil the high-order accuracy to some extent. Another method to discretize the stiff source term is to divide the time step in convection step into a series of smaller time steps.

To obtain high order accuracy time, we employ the explicit 3rd TVD Runge–Kutta scheme to discretize the stiff source term. However, great computational cost will generate if we use the same time steps in the whole computational domain in the reaction step. It is known that the stiffness only exists in the region near the detonation front and the severe time-step limitation disappears in the region far from the detonation. This reminds us that different time steps can be used in different areas to improve the efficiency.

In the splitting scheme, the reaction step can be expressed as

$$\frac{\mathrm{d}\rho_i}{\mathrm{d}t} = \omega_i, \tag{8}$$

where i represent the ith species. In Eq. (8), the magnitude of production rate ω_i can be used to indicate the stiffness of source term. The bigger ω_i is, the stiffer the Eq. (8) is and the smaller time-step should be used to maintain the stability of numerical methods. Here, we introduce an adaptive factor,

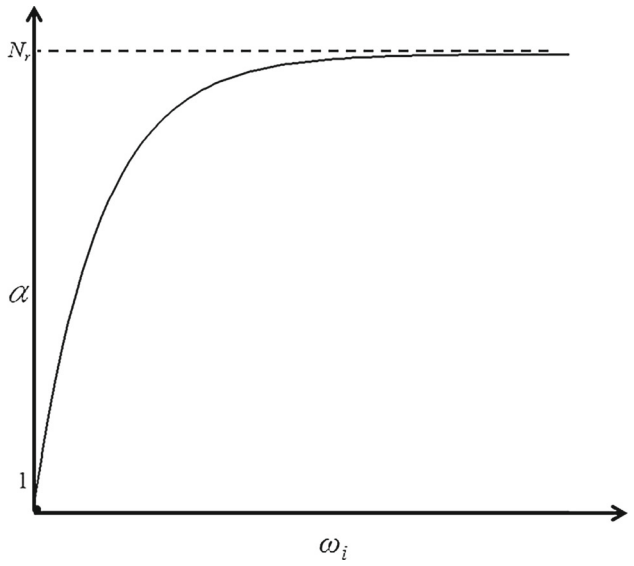

Fig. 1 Relationship between adaptive factor and production rate

which can be used to control the time-step for reaction adaptively. The adaptive time step for reaction has the following expression

$$\mathrm{d}t_R = \frac{\mathrm{d}t_c}{\alpha}, \tag{9}$$

where $\mathrm{d}t_c$ and α represents the convection time step and adaptive factor, respectively. The adaptive factor can be obtained in the following way

$$\alpha\left(\omega_i\right) = \left(N_r - 1\right)\left(1 - \mathrm{e}^{-A|\omega_i|}\right) + 1. \tag{10}$$

In the Eq. (10), N_r is the number of iterations in the traditional splitting scheme. A is a user-defined parameter, and we choose $A = 100$ in our computation. Our numerical tests will show that computation results are not sensitive to values of A. The relationship between α and ω_i is shown in Fig. 1. When the magnitude of ω_i is small, the source term is not stiff and the reaction time step is equal to the convection time step. When the magnitude of ω_i increases, the number of iterations become larger correspondingly, which maintains the stability of the numerical method.

3.2 Spatial discretization

To achieve high-order accuracy in smooth regions and non-oscillation transition for solution with discontinuities, an improved unstructured 3rd WENO method, which was developed for the multi-fluid flows in our previous work [41], is adopted to discretize the convection term.

Stencil for WENO reconstruction is shown in Fig. 2. The linear polynomial is reconstructed firstly on the sub-stencils.

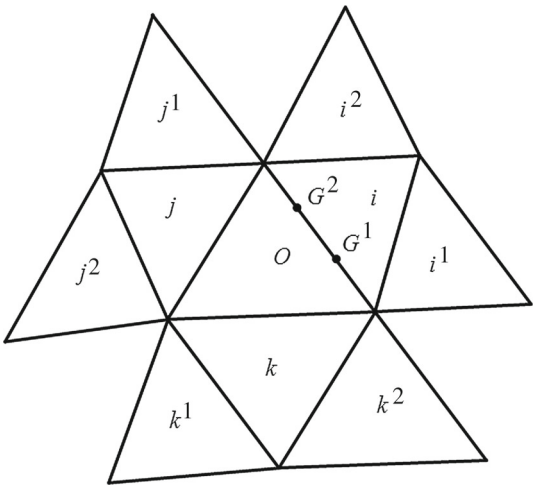

Fig. 2 Stencil for weighted essentially non-oscillatory reconstruction

After that, a quadratic polynomial is reconstructed from the combination of the linear polynomials. If discontinuities emerge, nonlinear weights are used to prevent numerical oscillation near discontinuities.

4 Numerical tests

In order to verify the proposed method for supersonic reactive flows on unstructured grids, four different numerical cases are tested.

4.1 1D C-J detonation wave with one-step chemical reaction model

In the first example, the simplified C-J detonation wave [14, 15] with one-step chemical reaction is tested. Initially, the computation domain is filled with burnt gas on the left-hand side and un-burnt gas on the right-hand side. The density, velocity, and pressure are given by

$$(\rho, u, p, z) = \begin{cases} (\rho_b, u_b, p_b, z_b), & x \le 10, \\ (1, 0, 1, 1), & x > 10. \end{cases} \tag{11}$$

The property of material and coefficients for chemical reaction are given as follows

$$\left(\gamma, q_0, A, B, T_{\text{ign}}\right) = (1.4, 25, 16418, 0.1, 15)\,, \tag{12}$$

States for the burnt gas can be obtained by the C-J relationship and the initial state for the un-burnt gas

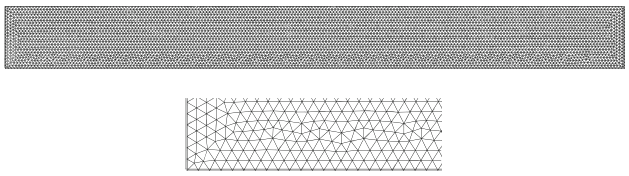

Fig. 3 Computational domain and grids for C-J detonation in one dimension ($h = 0.1$)

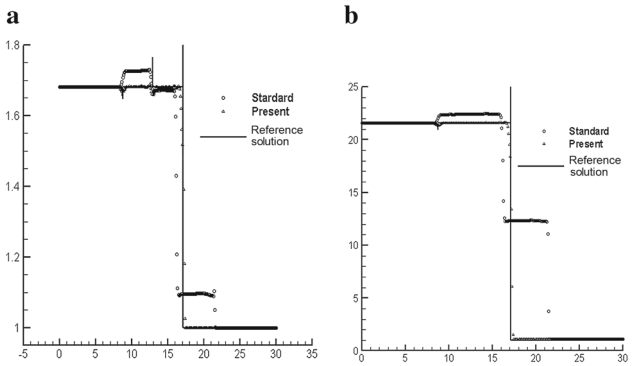

Fig. 4 Computed results for Example 4.1 at $t = 1.0$. **a** Density. **b** Pressure

$$\begin{aligned} p_b &= -b + (b^2 - c)^{1/2}, \\ \rho_b &= \rho_u \left[p_b\,(\gamma + 1) - p_u\right]/(\gamma\, p_b), \\ u_b &= S_{cj} - (\gamma\, p_b/\rho_b)^{1/2}\,, \\ b &= -\,p_u - \rho_u q_0\,(\gamma - 1)\,, \\ c &= p_u^2 + 2\,(\gamma - 1)\,p_u \rho_u q_0/(\gamma + 1), \\ S_{cj} &= \left[\rho_u u_u + (\gamma\, p_b \rho_b)^{1/2}\right]/\rho_u, \end{aligned} \tag{13}$$

where S_{cj} is the speed of the C-J detonation wave. In this example, $S_{cj} = 7.1247$.

In this example, the computational domain is $[0, 30] \times [0, 3]$, as shown in Fig. 3. The size of the computational cell is $h = 0.1$. Initially, the discontinuity is located at $x = 10$. At the final time $t = 1.0$, the density and pressure profile along the center line of $y = 1.5$ using the present method and standard method is shown in Fig. 4. The reference solution is computed by the standard WENO scheme of fifth order with 15,000 grids in the x-direction. From the computational results, we can find that the detonation wave computed by the standard method has moved to $x = 21.5$, which is obviously larger than the reference solution $x = 17.12$. However, the results using the present method agree well with the reference solution.

4.2 2D detonation waves with one-step chemical reaction model

Consider a 2D channel, the upper and lower boundaries are solid walls. The computational domain is $[0, 0.015] \times [0,$

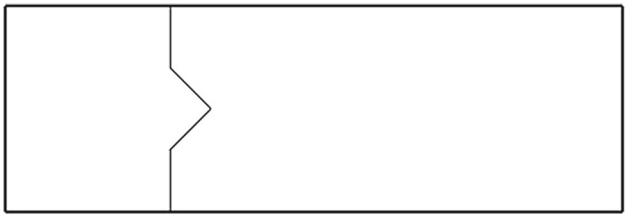

Fig. 5 Computational domain and initial condition in 2D detonation wave

0.005], as shown in Fig. 5. The domain is discretized by unstructured grids with $h = 2.5 \times 10^{-5}$. The initial conditions are

$$(\rho, u, p, z) = \begin{cases} \left(\rho_b, 8.162 \times 10^4, 0, p_b, 0\right), & x < \xi\,(y), \\ \left(1.201 \times 10^{-3}, 0, 0, 8.321 \times 10^5, 1\right), & x \geq \xi\,(y), \end{cases} \tag{14}$$

where

$$\xi\,(y) = \begin{cases} 0.004, & |y - 0.0025| \geq 0.001, \\ 0.005 - |y - 0.0025|, & |y - 0.0025| < 0.001. \end{cases} \tag{15}$$

In this example [17,18], a moving detonation wave travels from left to right in the channel. One important feature of this problem is the appearance of triple points, which has been discussed in detail in Ref. [43]. The parameters for burnt gas can be obtained by Eq. (13) in Sect. 4.1. The chemical reaction is modeled by the Heaviside form with the following coefficients

$$\left(\gamma, q_0, Da, T_{\text{ign}}\right) = \left(1.4, 5.196 \times 10^9, 5.825 \times 10^9, 8.085 \times 10^8\right). \tag{16}$$

Figure 6 show temperature contours computed by the present method at different times from $t = 0$ to $t = 6 \times 10^{-8}$. The evolution process of detonation wave with triple points can be observed clearly. In this example, the reference solution is from Ref. [18], which is calculated by the MUSCL scheme using structured grids. At the final time $t = 6 \times 10^{-8}$, we compared solutions using the present method and the solution using standard method in one-dimensional cross section at $y = 0.0025$. As shown in Fig. 7, this method is able to capture the correct propagation speed of the detonation wave exactly even in coarse grids, while the standard method produces spurious numerical results, in which detonation wave travels faster than the reference solution.

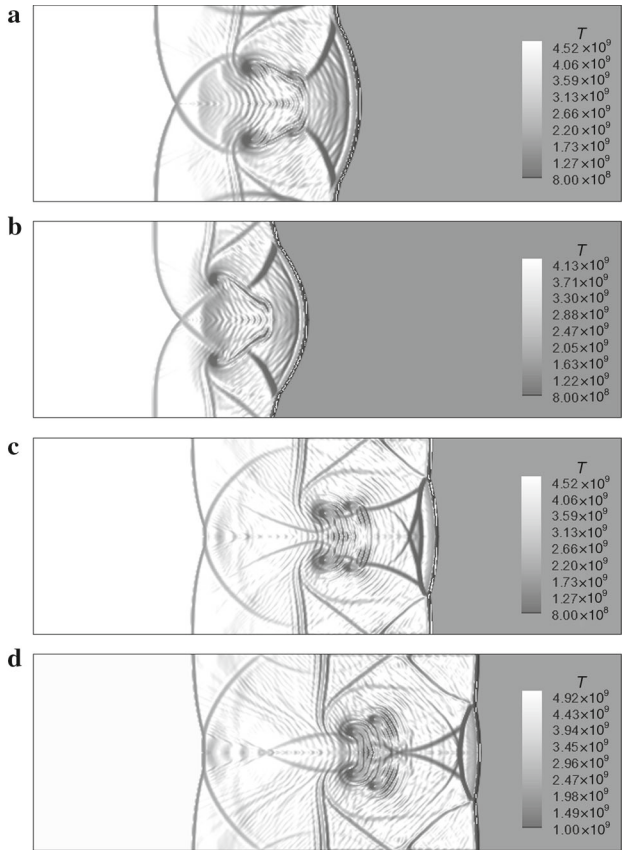

Fig. 6 Temperature contours at different times for 2D detonation wave using the third order accurate WENO scheme. From top to bottom: **a** $t = 2 \times 10^{-8}$. **b** $t = 3 \times 10^{-8}$. **c** $t = 5 \times 10^{-8}$. **d** $t = 6 \times 10^{-8}$

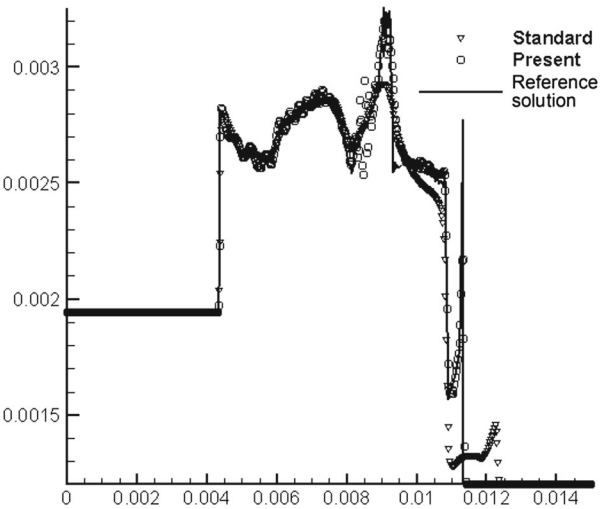

Fig. 7 Comparison of different schemes along the cross section of $y = 0.0025$

4.3 Interaction of detonation wave and shock wave

This example is taken from Refs. [18,30]. In this numerical test, a detonation and shock wave sweep a contact surface of

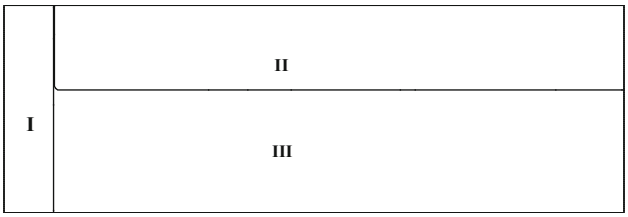

Fig. 8 Computational domain and initial condition for detonation and shock interaction

un-burnt gas. The computation domain can be divided into three parts, as shown in Fig. 8. The size for unstructured grids is $h = 0.02$. Initial conditions for each part are as follows

$$(\rho, u, v, p) = \begin{cases} (2, 10, 0, 40), & x \le 0.5, \\ (1, 0, 0, 1), & x > 0.5, \end{cases} \tag{17}$$

$$\begin{aligned} &\left(z_{H_2}, z_{O_2}, z_{OH}, z_{H_2O}, z_{N_2}\right) \\ &= \begin{cases} (0, 0, 0.17, 0.63, 0.2), & x \le 0.5, \\ (0, 0, 0.17, 0.63, 0.2), & x > 0.5,\ y \ge 1.2, \\ (0.08, 0.72, 0, 0, 0.2), & x > 0.5,\ y < 1.2. \end{cases} \end{aligned} \tag{18}$$

A reacting model, which consists of five species and two reactions is adopted. The species of N_2 is added to the mixture as dilution gas. Chemical reaction equations can be written in the following expression

$$H_2 + O_2 \rightarrow 2OH, \quad 2OH + H_2 \rightarrow 2H_2O, \tag{19}$$

The chemical reaction is modeled by the Heaviside form and the chemical parameters used in the computation are given by

$$\begin{aligned} &\left(\gamma, T_{ign}^1, Da^1, T_{ign}^2, Da^2\right) = \left(1.4, 1.5, 10^5, 10, 2 \times 10^4\right), \\ &\left(q_{H_2}, q_{O_2}, q_{OH}, q_{H_2O}, q_{N_2}\right) = (0, 0, -50, -100, 0), \\ &\left(W_{H_2}, W_{O_2}, W_{OH}, W_{H_2O}, W_{N_2}\right) = (2, 32, 17, 18, 28). \end{aligned} \tag{20}$$

Figure 9 shows the temperature contours computed using the present method at different times from $t = 0$ to $t = 3.0$. We can find that the detonation wave travels faster than the shock wave. The profiles along $y = 1$ at $t = 3.0$ are also plotted in Fig. 10. From the profile for pressure, temperature and mass fraction, we can see that the present results agree well with the reference ones.

4.4 1D detonation wave with detailed chemical reaction for thermally perfect gas

In the last example, the mixture belongs to thermally perfect gas and similar examples can be found in Refs. [27,44–48].

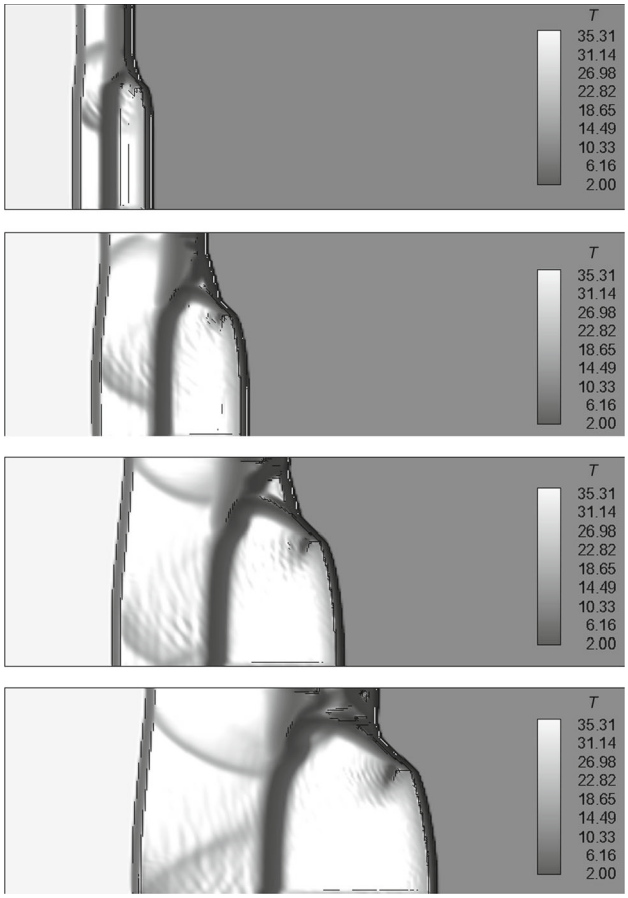

Fig. 9 Temperature contours for detonation and shock interaction at different times: $t = 0.075, 0.15, 0.225, 0.3$

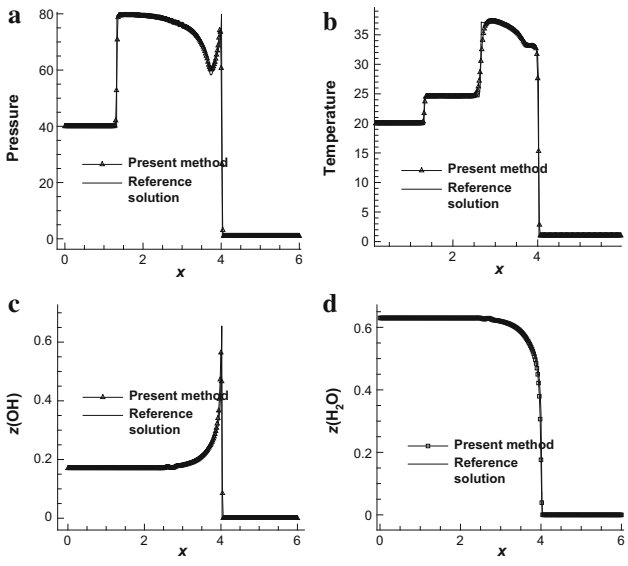

Fig. 10 Solution using the present method along the cross section of $y = 1$. **a** Pressure. **b** Temperature. **c** Mass fraction of OH. **d** Mass fraction of H_2O

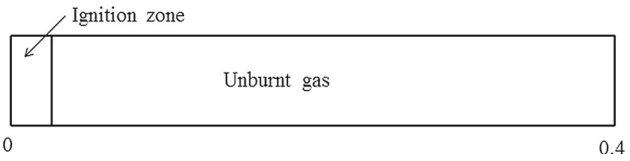

Fig. 11 Computational domain and boundary condition for multi-species detonation problem with detailed chemical reaction

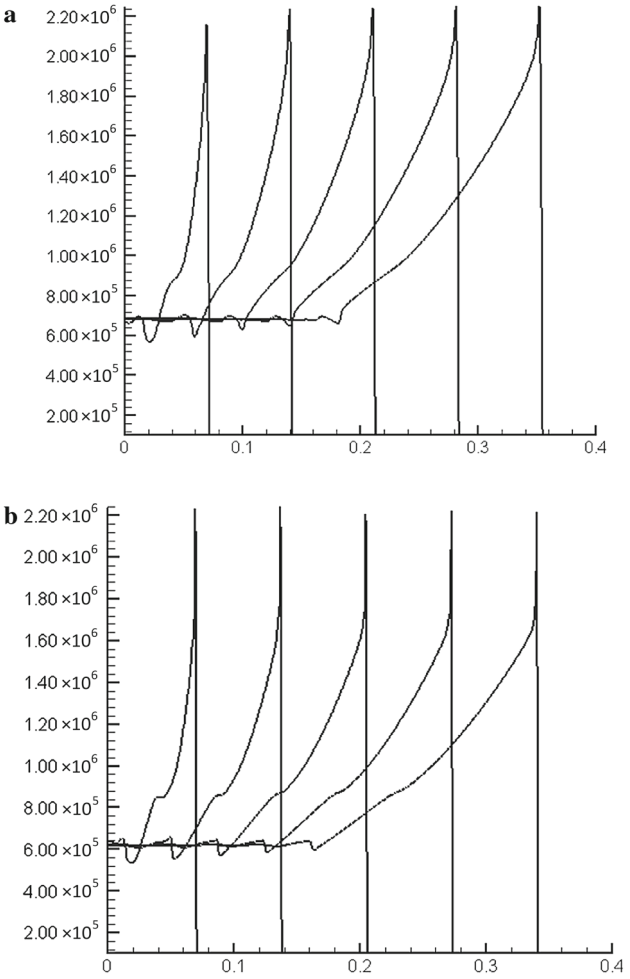

Fig. 12 Pressure contours along the cross section of $y = 0.02$. **a** Second order scheme. **b** Third order WENO scheme

The mole concentration ratio of the $H_2/O_2/Ar$ gas mixture was 2:1:7, with initial pressure 6670 Pa and temperature 298 K. In this example, an 8-species and 19-step reaction mechanism for hydrogen-oxygen combustion [49] is used. Reacting species are H, O, H_2, OH, H_2O, O_2, HO_2, and H_2O_2. The specific heat capacities and enthalpies for each species can be found in the JANAF tables [50]. The computational domain is shown in Fig. 11, whose boundary conditions for the left side, upper and lower sides are solid walls. The size of unstructured grids is $h = 5 \times 10^{-4}$ m. Detonation wave is generated by igniting the mixture gas in the left (width of 0.1 m) with a high initial pressure and temperature as 18 P_0 and $18T_0$.

Table 1 CPU time using different methods

	Value of A	CPU time/s
Adaptive method	10^2	7.5×10^3
	10^3	8.2×10^3
	10^4	8.2×10^3
	10^5	8.3×10^3
	10^6	8.3×10^3
Traditional splitting method		1.4×10^4

The pressure contours at different times along the cross section of $y = 0.02$ are shown in Fig. 12. In this example, the theoretical speed of detonation wave is 1722 m/s. The speed of detonation using the second order finite element method is 1770 m/s with relative error of 2.7%. However, in our numerical simulation, the speed of detonation using the present method is 1690 m/s with relative error of -1.9%. From the pressure profile in Fig. 12, it is easy to see that the third-order WENO scheme can obtain sharper results than the second order scheme.

We also compared the CPU time using different methods, as shown in Table 1. It is easy to find that the CPU time is not sensitive to the magnitude of A and all the cases that use adaptive method cost about a half time than the traditional one, which means that the proposed method can reduce the computational cost effectively.

5 Conclusions

An effective unstructured 3rd order FVM for supersonic reactive flows is proposed in this article. In our proposed method, the convection step and reaction step are solved separately. In the reaction step, an adaptive time-step method is presented. In the convection step, a third-order accurate unstructured WENO reconstruction is adopted. Numerical results show that present method can capture the correct propagation speed of the detonation wave exactly and obtain better detonation profile than the second order method. In addition, the proposed method can greatly reduce the computational cost compared with the traditional splitting method.

Acknowledgements The project was supported by the National Natural Science Foundation of China (Grants 51476152, 11302213, and 11572336). The authors wish to thank Jun Meng, Li Liu, Jun Peng, Shengping Liu and Guangli Li for helpful discussions. Special thank goes to Prof. Yiqing Shen and Prof. Xinliang Li of the Institute of Mechanics CAS for their suggestions and help.

References

1. Roy, G.D.: Pulse detonation propulsion: challenges, current status, and future perspective. Prog. Energy Combust. **30**, 545–672 (2004)
2. Geßner, T.: Dynamic mesh adaption for supersonic combustion waves modeled with detailed reaction mechanisms. [Ph.D. Thesis], Technical University Dresden, German (2001)
3. Fedkiw, R.P., Merriman, B., Osher, S.: High accuracy numerical methods for thermally perfect gas flows with chemistry. J. Comput. Phys. **132**, 175–190 (1997)
4. Togashi, F., Löhner, R., Tsuboi, N.: Numerical simulation of H_2/air detonation using unstructured mesh. Shock Waves **192**, 151–162 (2009)
5. Ju, Y.: Recent progress and challenges in fundamental combustion research. Adv. Mech. **44**, 1142–1157 (2014)
6. Chapman, D.L.V.I.: On the rate of explosion in gases. Lond. Edinb. Dublin Philos. Mag. J. Sci. **47**, 90–104 (1899)
7. Jouguet, E.: On the propagation of chemical reactions in gases. J. Math. Pureset Appl. **1**, 347–425 (1905)
8. Zeldovich, Y.B.: On the theory of the propagation of detonation in gaseous systems. Tech. Memos. Nat. Adv. Comm. Aeronaut. **1950**, 1261 (1950)
9. Von Neuman, J.: Theory of Detonation Waves. Institute for Advanced Study, Princeton (1942)
10. Döring, W.: On detonation processes in gases. Ann. Phys. **43**, 421–436 (1943)
11. Bao, W., Jin, S.: The random projection method for hyperbolic conservation laws with stiff reaction terms. J. Comput. Phys. **163**, 216–248 (2000)
12. Bao, W., Jin, S.: The random projection method for stiff detonation capturing. SIAM J. Sci. Comput. **23**, 1000–1026 (2001)
13. Bao, W., Jin, S.: The random projection method for stiff multispecies detonation capturing. J. Comput. Phys. **178**, 37–57 (2002)
14. Helzel, C., Leveque, R.J., Warnecke, G.: A modified fractional step method for the accurate approximation of detonation waves. SIAM J. Sci. Comput. **22**, 1489–1510 (2000)
15. Tosatto, L., Vigevano, L.: Numerical solution of under-resolved detonations. J. Comput. Phys. **227**, 2317–2343 (2008)
16. Dumbser, M., Enaux, C., Toro, E.F.: Finite volume schemes of very high order of accuracy for stiff hyperbolic balance laws. J. Comput. Phys. **227**, 3971–4001 (2008)
17. Wang, W., Shu, C.W., Yee, H.C., et al.: High order finite difference methods with subcell resolution for advection equations with stiff source terms. J. Comput. Phys. **231**, 190–214 (2012)
18. Zhang, B., Liu, H., Chen, F.: The equilibrium state method for hyperbolic conservation laws with stiff reaction terms. J. Comput. Phys. **263**, 151–176 (2014)
19. Taki, S., Fujiwara, T.: Numerical analysis of two-dimensional nonsteady detonations. AIAA J. **16**, 73–77 (1978)
20. Lefebvre, M.H., Oran, E.S., Kailasanath, K.: Computations of Detonation Structure: The Influence of Model Input Parameters. Naval Research Lab, Washington, DC (1992)
21. Sichel, M., Tonello, N.A., Oran, E.S., et al.: A two-step kinetics model for numerical simulation of explosions and detonations in H_2–O_2 mixtures. R. Soc. **458**, 49–82 (2002)
22. Colella, P., Majda, A., Roytburd, V.: Theoretical and numerical structure for reacting shock waves. SIAM J. Sci. Comput. **7**, 1059–1080 (1986)
23. LeVeque, R.J., Yee, H.C.: A study of numerical methods for hyperbolic conservation laws with stiff source terms. J. Comput. Phys. **86**, 187–210 (1990)
24. Bussing, T.R.A., Murman, E.M.: Finite-volume method for the calculation of compressible chemically reacting flows. AIAA J. **26**, 1070–1078 (1988)
25. Gnoffo, P.A.: An upwind-biased, point-implicit relaxation algorithm for viscous, compressible perfect-gas flows. NASA Tech. Rep. **90**, 17–42 (1990)
26. Zhong X.: New high-order semi-implicit Runge–Kutta schemes for computing transient nonequilibrium hypersonic flow. In: 30th Thermophysics Conference, New York, August 4–14 (1995)
27. Oran, E.S., Weber, J.W., Stefaniw, E.I., et al.: A numerical study of a two-dimensional H_2–O_2–Ar detonation using a detailed chemical reaction model. Combust. Flame **113**, 147–163 (1998)
28. Xiao, X., Edwards, J.R., Hassan, H.A., et al.: Inflow boundary conditions for hybrid large eddy/Reynolds averaged Navier–Stokes simulations. AIAA J. **41**, 1481–1489 (2003)
29. Shen, Y., Zha, G.: Application of low diffusion E-CUSP scheme with high order WENO scheme for chemical reacting flows. In: The 40th Fluid Dynamics Conference and Exhibit, Chicago, June 28–30 (2010)
30. Taylor, B.D., Kessler, D.A., Gamezo, V.N., et al.: Numerical simulations of hydrogen detonations with detailed chemical kinetics. Proc. Combust. Inst. **34**, 2009–2016 (2013)
31. Billet, G., Ryan, J., Borrel, M.: A Runge Kutta discontinuous Galerkin approach to solve reactive flows on conforming hybrid grids: the parabolic and source operators. Comput. Fluids **95**, 98–115 (2014)
32. Lv, Y., Ihme, M.: Discontinuous Galerkin method for multicomponent chemically reacting flows and combustion. J. Comput. Phys. **270**, 105–137 (2014)
33. Dumbser, M., Castro, M., Parés, C., et al.: ADER schemes on unstructured meshes for non-conservative hyperbolic systems: applications to geophysical flows. Comput. Fluids **38**, 1731–1748 (2009)
34. Dumbser, M., Zanotti, O.: Very high order PNPM schemes on unstructured meshes for the resistive relativistic MHD equations. J. Comput. Phys. **228**, 6991–7006 (2009)
35. Titarev, V.A., Tsoutsanis, P., Drikakis, D.: WENO schemes for mixed-element unstructured meshes. Commun. Comput. Phys. **8**, 585–609 (2010)
36. Zhang, Y.T., Shu, C.W.: Third order WENO scheme on three dimensional tetrahedral meshes. Commun. Comput. Phys. **5**, 836–848 (2009)
37. Zhang, Y., Shu, C.: High-order WENO Sschemes for Hamilton–Jacobi equations on triangular meshes. SIAM J. Sci. Comput. **24**, 1005–1030 (2003)
38. Togashi, F., Löhner, R., Tsuboi, N.: Numerical simulation of H_2/air detonation using unstructured mesh. Shock Waves **19**, 151–162 (2009)
39. Wang, Z.J.: High-order methods for the Euler and Navier–Stokes equations on unstructured grids. Prog. Aerosp. Sci. **43**, 1–41 (2007)
40. Ekaterinaris, J.A.: High-order accurate, low numerical diffusion methods for aerodynamics. Prog. Aerosp. Sci. **41**, 192–300 (2005)
41. Harten, A., Engquist, B., Osher, S., et al.: Uniformly high order accurate essentially non-oscillatory schemesIII. J. Comput. Phys. **71**, 231–303 (1987)
42. Liu, X.D., Osher, S., Chan, T.: Weighted essentially non-oscillatory schemes. J. Comput. Phys. **115**, 200–212 (1994)
43. Jiang, G.S., Shu, C.W.: Efficient implementation of weighted ENO schemes. J. Comput. Phys. **126**, 202–228 (1996)
44. Cockburn, B., Karniadakis, G.E., Shu, C.W.: The Development of Discontinuous Galerkin Methods. Springer, Berlin (2000)
45. Wang, Z.J.: Spectral (finite) volume method for conservation laws on unstructured grids basic formulation. J. Comput. Phys. **178**, 210–251 (2002)
46. Zheng, H., Zhao, W.G.: An improved unstructured WENO method for compressible multi-fluids flow. In. J. Numer. Methods Fluids **82**, 113–129 (2016)
47. Stull, D., Prophet, H.: JANAF Thermo Chemical Tables, 2nd edn. NSRDS-NBS37, Washington (1971)

48. Kailasanath, K., Oran, E.S., Boris, J.P.: Determination of detonation cell size and the role of transverse waves in two-dimensional detonations. Combust. Flame **61**, 199–209 (1985)
49. Hu, Z., Mu, Q., Zhang, D., et al.: Numerical simulation of gaseous detonation wave propagation through bends with a detailed chemical reaction model. Chin. J. Comput. Phys. **21**, 408–414 (2004)
50. Lv, Y., Ihme, M.: Development of discontinuous Galerkin method for detonation and supersonic combustion. In: 51st AIAA Aerospace Sciences Meeting, Grapevine, January 7–10 (2013)
51. Deiterding, R., Bader, G.: High-Resolution Simulation of Detonations with Detailed Chemistry. In: Analysis and Numeric for Conservation Laws, Berlin Heidelberg, May 4–12 (2005)
52. Eckett, C.A.: Numerical and Analytical Studies of the Dynamics of Gaseous Detonations [Ph.D. Thesis], California Institute of Technology, America (2000)
53. Deiterding, R.: Parallel Adaptive Simulation of Multi-Dimensional Detonation Structures. [Ph.D. Thesis], Branderburg University of Technology Cottbus, German (2003)
54. Li, J., Zhao, Z., Kazakov, A., et al.: An updated comprehensive kinetic model of hydrogen combustion. Int. J. Chem. Kinet. **36**, 566–575 (2004)
55. Stull, D.R., Prophet, H.: JANAF thermo chemical tables. Technical report, U. S. Department of Commerce (1971)
56. Hu, C., Shu, C.W.: Weighted essentially non-oscillatory schemes on triangular meshes. J. Comput. Phys. **150**, 97–127 (1971)
57. Dumbser, M., Käser, M., Titarev, V.A., et al.: Quadrature-free non-oscillatory finite volume schemes on unstructured meshes for nonlinear hyperbolic systems. J. Comput. Phys. **226**, 204–243(2007)
58. Ivan, L.: High-order central ENO finite-volume scheme for hyperbolic conservation laws on three-dimensional cubed-sphere grids. J. Comput. Phys. **12**, 157–182 (2015)
59. Ivan, L., Clinton, P.T.: High-order solution-adaptive central essentially non-oscillatory (CENO) method for viscous flows. J. Comput. Phys. **11**, 830–862 (2014)
60. Billet, G., Ryan, J., Borrel, M.: A Runge Kutta discontinuous Galerkin approach to solve reactive flows on conforming hybrid grids: the parabolic and source operators. Comput. Fluids **1**, 98–115 (2014)
61. Billet, G., Ryan, J., Borrel, M.: A Runge Kutta discontinuous Galerkin approach to solve reactive flows on conforming hybrid grids: the parabolic and source operators. Comput. Fluids **23**, 98–115 (2014)
62. Ren, Z.: Dynamic adaptive chemistry with operator splitting schemes for reactive flow simulations. J. Comput. Phys. **263**, 19–36 (2014)
63. Cai, X., Liang, J., Lin, Z., et al.: Adaptive mesh refinement-based numerical simulation of detonation initiation in supersonic combustible mixtures using a hot jet. J. Aerosp. Eng. **28**, 1–15 (2015)
64. Florian, E., Klaus, G., Sattelmayer, T.: Numerical simulation of the deflagration to detonation transition in inhomogeneous mixtures. J. Combust. **31**, 1–15 (2014)
65. Zhou, R., Wu, D., Wang, J.: Progress of continuously rotating detonation engines. Chin. J. Aeronaut. **29**, 15–29 (2016)
66. Qing, Y., Zhang, X.: Discontinuous Galerkin immersed finite element methods for parabolic interface problems. J. Comput. Appl. Math. **1**, 127–139 (2016)
67. Assyr, A., Huber, M.E.: Discontinuous Galerkin finite element heterogeneous multiscale method for advection–diffusion problems with multiplescales. Numer. Math. **126**, 589–633 (2014)